Light absorption properties of cooled soot

Coderre, Adam R.; Thomson, Kevin A.; Snelling, David R.; Johnson, Matthew R.

Proceedings of Combustion Institute - Canadian Section Spring Technical Meeting, 2009, 2009-05

Proceedings of Combustion Institute – Canadian Section
Spring Technical Meeting
Université de Montréal, Québec
May 11-13, 2009

Light Absorption Properties of Cooled Soot

Adam R. Coderre[a], Kevin A. Thomson[b], David R. Snelling[b], Matthew R. Johnson[a*]

[a] *Department of Mechanical and Aerospace Engineering, Carleton University, 1125 Colonel By Drive, Ottawa, Ontario K1S 5B6*
[b] *Combustion Group, Institute for Chemical Process and Environmental Technology, National Research Council of Canada, 1200 Montreal Road, Ottawa, Ontario K1A 0R6*

1. Introduction

Optical methods for the measurement of particulate matter have gained popularity in the combustion community due to their robustness, speed, and non-intrusive nature. In particular, laser-induced incandescence (LII) has been the subject of worldwide research and development, and is a maturing technology capable of measuring spatially- and temporally-resolved soot volume fraction (f_v) as well as primary particle diameter (d_p) in a wide range of applications [1]. However, the accuracy of all optical methods, including LII, hinge on the accuracy to which the optical properties of soot are known. Indeed, the uncertainty in the optical properties of soot is one of the dominant sources of uncertainty for such diagnostics (e.g. [2]).

The optical properties of soot have seen much attention in the past, and the methods used to obtain them are as widely varied as the results. It is often the case that values reported in literature are used generically, despite the specific nature of the experiments used to obtain these data. The flaring of solution gas during oil and natural gas production is implicated as a significant source of particulate matter emissions, though few studies have considered soot from flames burning methane, the primary constituent of solution gas. In addition, the majority of measurements of soot optical properties have been made within the flame or shortly thereafter, which do not necessarily represent soot found in smokestack or tailpipe emissions, nor aged soot relevant to atmospheric measurements. Finally, the spectral variation in optical properties is crucial to determining particle temperatures by pyrometry, which is key to the analysis of LII signals. The present work is an effort to address these issues by extending the body of knowledge on soot optical properties to include spectrally-resolved absorption properties of cooled soot from a methane flame.

2. Experimental

The soot absorption refractive index function, *E(m)*, is a key parameter in absorption-based optical diagnostics such as LII. The Rayleigh-Debye-Gans approximation for polydisperse fractal aggregates (RDG-PFA) states that *E(m)*, the soot volume fraction, f_v, the volumetric extinction coefficient, $K_{ext,\lambda}$, and the scatter to absorption ratio, $\rho_{sa,\lambda}$, are related according to Equation (1). Thus, these latter three parameters needed to be determined in order to calculate *E(m)*. The experimental methodology used to determine these parameters has been discussed in our previous work [3], and is described only briefly here.

$$E(m)_\lambda = \frac{K_{ext,\lambda}\lambda}{6\pi(1+\rho_{sa,\lambda})f_v} \quad (1)$$

* Corresponding author: Matthew_Johnson@carleton.ca

Soot was generated using an inverted-flame burner, designed after the work of Stipe *et al.* [4], capable of producing a highly stable and repeatable soot aerosol at near-ambient temperatures. The burner is described in detail in our previous work [5]. A total of twelve burner conditions were studied, with three main variables of interest: dilution ratio, dilution temperature, and dilution gas. Three different dilution rates were sampled for three different dilution air temperatures each. One of those conditions was also selected to be run with nitrogen as the diluent rather than air, to investigate post-flame oxidation effects. Finally, a slightly globally-rich condition was run with both air and nitrogen diluents, so that no excess oxygen was present in the exhaust stream and thus no post-flame soot oxidation could occur. The twelve burner conditions are summarized in Table 1. Global equivalence ratios were determined assuming complete (ideal) combustion of methane with air consisting of 21% oxygen, according to $\phi = (2 \cdot Q_{fuel}) / (0.21 \cdot Q_{air})$, where Q is the volume flow rate in standard litres per minute (SLPM), and dilution ratio (DR) was defined as the volumetric ratio of dilution gas to combustion products, which for methane is equivalent to $DR = Q_{dil} / (Q_{fuel} + Q_{air})$. The labelling scheme is somewhat arbitrary, though it does carry some meaning: series C, D, and E indicate the varying dilution rate, and each numerical suffix represents a different dilution inlet temperature (e.g. C1 indicates 50 SLPM of dilution air at 100°C, D2 indicates 40 SLPM dilution at 60°C, etc.). The B series is the fuel-rich condition, the first with air as the diluent and the second with nitrogen. A1 corresponds to condition C3, only with nitrogen as the diluent.

Table 1**:** Summary of burner conditions

Label	Q_{fuel} **[SLPM]**	Q_{air} **[SLPM]**	Q_{dil} **[SLPM]**	**Diluent (N_2 / air)**	T_{dil} **[°C]**	ϕ **(global)**	***DR*** **(vol.)**
A1	1.2	15	50	N_2	25	0.76	3.1
B1	1.4	13	50	air	25	1.03	3.5
B2	1.4	13	50	N_2	25	1.03	3.5
C1	1.2	15	50	air	100	0.76	3.1
C2	1.2	15	50	air	60	0.76	3.1
C3	1.2	15	50	air	25	0.76	3.1
D1	1.2	15	40	air	100	0.76	2.5
D2	1.2	15	40	air	60	0.76	2.5
D3	1.2	15	40	air	25	0.76	2.5
E1	1.2	15	30	air	100	0.76	1.9
E2	1.2	15	30	air	60	0.76	1.9
E3	1.2	15	30	air	25	0.76	1.9

Soot volume fraction was determined via gravimetric analysis, whereby soot was collected on a filter from some known volume of exhaust gas, V, and weighed to determine the mass of soot, m_s. Assuming a soot density, ρ_s, of 1.89 g/cm^3 from literature [6-9], the soot volume could then be found. The soot volume fraction was then simply the ratio of the sampled soot volume to the sampled gas volume, corrected for temperature change if necessary; mathematically, this is expressed in Equation (2), where T_s is the soot/exhaust gas temperature at the burner exit and T_∞ is the gas temperature at the point of measurement (ambient):

$$f_v = \frac{m_s}{\rho_s V} \frac{T_s}{T_\infty} \tag{2}$$

Spectrally-resolved volumetric extinction coefficients were determined using diffuse spectral line-of-sight attenuation. This method was discussed in detail by Thomson et al. [10] at the 2008 Spring Technical Meeting in Toronto. Briefly, line of sight attenuation is an extinction measurement where the incident ($I_{\lambda 0}$) and transmitted light (I_λ) are ratioed to obtain the transmissivity, τ. Three images were collected for each measurement, which were referred to as *plume*, *lamp*, and *dark*, using a diffuse broadband ('white') light source and an imaging spectrometer as the detector. Two wavelength ranges were measured separately, with a combined spectrum of 450-950 nm. The dark image was taken with the light source off and the plume blocked, to measure ambient light and so-called dark counts on the CCD. The lamp image was taken with the lamp on and the plume blocked, to measure the incident light. Finally, the plume image was

taken with the lamp on and the plume flowing, to measure the transmitted light. The transmissivity of the plume, and thereby the line-integrated extinction coefficient, was then found according to

$$\tau = \frac{plume - dark}{lamp - dark} = \frac{I_\lambda}{I_{\lambda 0}} = \exp\left(- \int_{-\infty}^{\infty} K_{ext,\lambda}(s)\, ds \right), \tag{3}$$

where s is the position along the optical path. The uniformity of the plume was verified by tomographic inversion to obtain a radial transmissivity profile, and only the centre portion of the plume was used to determine $K_{ext,\lambda}$ in order to avoid any entrainment effects around the edges of the open plume.

The scatter-to-absorption ratio was calculated using the Rayleigh-Debye-Gans approximation for polydisperse fractal aggregates (RDG-PFA), which required knowledge of the soot physical structure. This morphological information was acquired by a combination of scanning and transmission electron microscopy (SEM, TEM), and image processing followed the procedure given by Brasil *et al.* [11]. Further details of the analysis are described in [12]. A detailed uncertainty analysis was carried out to estimate the 95% confidence intervals associated with these measurements. The results of this analysis are expressed as uncertainty bars in the graphs presented in the following sections.

LII data were taken using the apparatus described by Snelling *et al*. [1], and re-analyzed using various values of *E(m)*, including the spectrally-resolved values found in the present work. The results of this comparison are discussed below.

3. Results and Discussion

Spectrally-resolved values for the soot absorption refractive index function over the range of 450-950 nm were determined at 25-nm increments for the twelve burner conditions given in Table 1, and are presented in Figure 1(a). Note that there is some discontinuity present in the results between lower-wavelength and higher-wavelength values for the same condition; this is an artifact resulting from the LOSA measurements, where these two wavelength ranges were measured separately.

Another common representation of absorption properties is the mass-normalized absorption cross-section (MAC). As seen in Equation (4), this form accounts for the scatter correction, but loses the wavelength term seen in Equation (1). MAC data is presented in Figure 1(b).

$$\mathrm{MAC} = \frac{K_{ext,\lambda}}{\rho_s (1 + \rho_{sa}) f_v} \tag{4}$$

The results were plotted against several relevant morphological and experimental parameters in an attempt to better understand the variability. However, correlation was found with only one, somewhat obvious, parameter: the wavelength of light. The lack of variability among the tested conditions suggests that, within uncertainty limits, the parameters varied (T_{dil}, Q_{dil}, dilution gas) have little effect on the resultant optical properties of soot. If the measurements made for the twelve burner conditions studied here are considered repeated measurements of the same values, the spread in their results can be seen as a measure of the precision error. The results of such a treatment, in terms of *E(m)*, can be seen in Figure 2(a). The relatively narrow uncertainty bars seen in the figure suggest that it is indeed reasonable to treat the twelve conditions as repeated measurements. Under this assumption, a wavelength-dependent soot absorption function could be defined for more generalized use at a range of conditions. Figure 2(a) also serves to clarify the wavelength dependence of *E(m)* seen in the present work, the consistency of which is indicative of a universal trend.

This wavelength trend was investigated further by plotting the relative *E(m)*, in which each wavelength range of each condition is normalized separately by the maximum value in that range. These results can be seen in Figure 2(b), which shows a high degree of consistency among conditions. Data for the two conditions in the fuel-rich "B" series are possible exceptions, showing a difference in slope at the lower wavelengths compared to the other conditions. That this difference in slope was seen only in the tests done at globally rich conditions could indicate that flame condition could have some effect on *E(m)*.

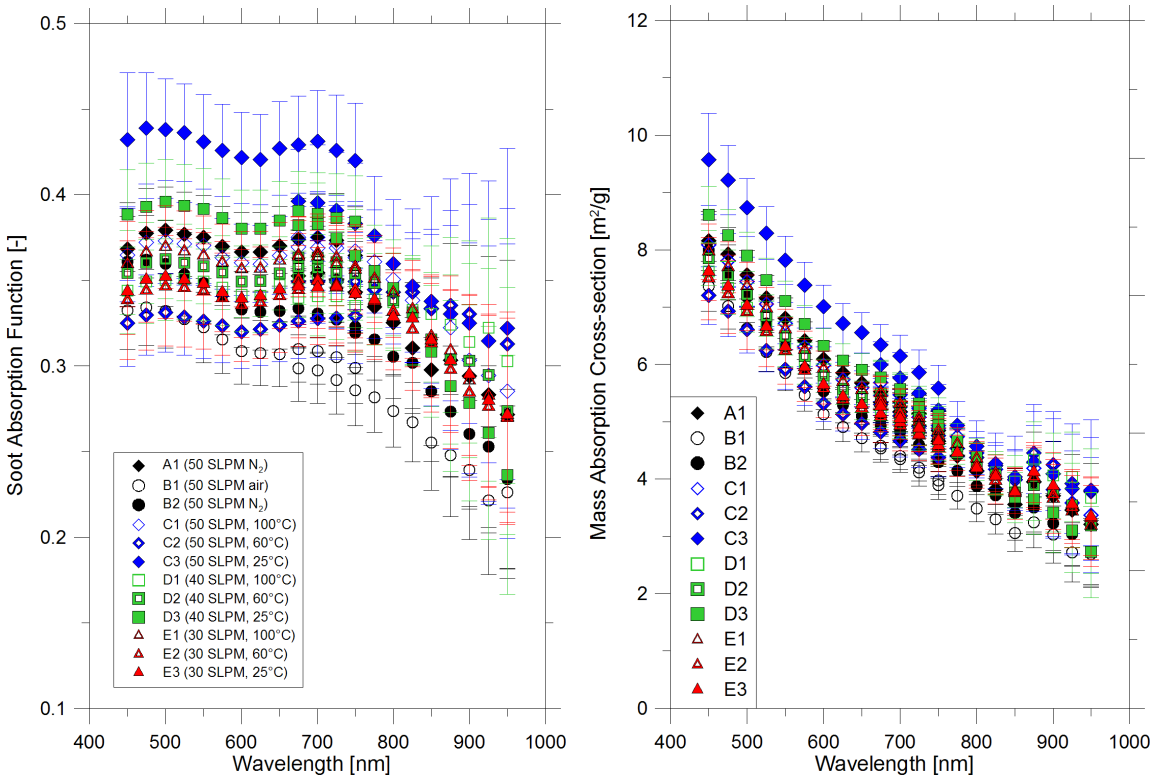

Figure 1: Results for the twelve burner conditions studied in this work, in terms of (a) *E(m)* and (b) MAC

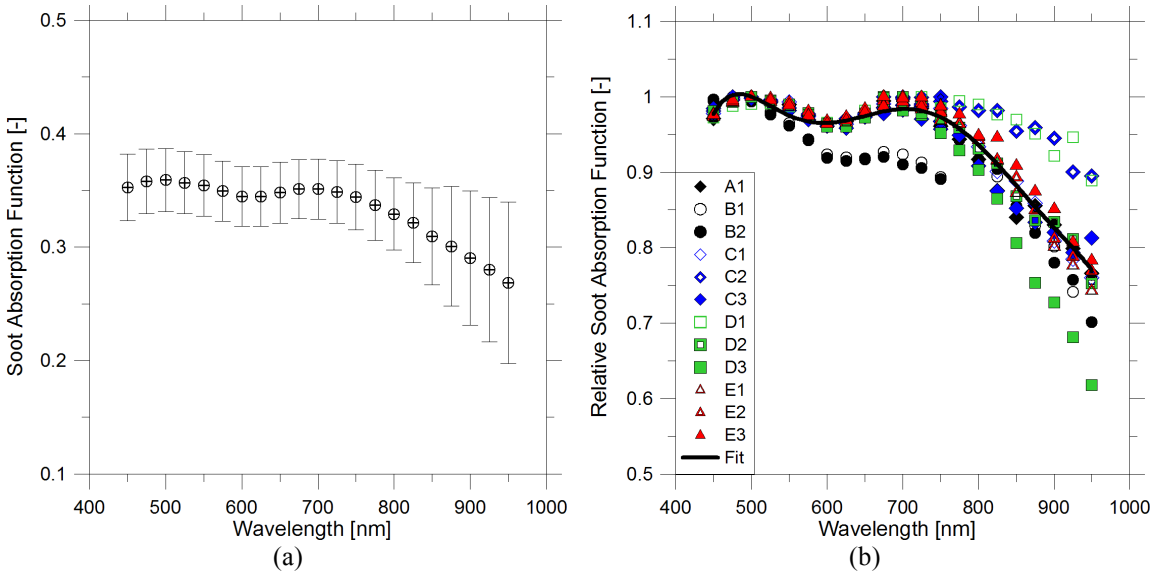

Figure 2: Variation with wavelength: (a) *E(m)* results, treating the twelve conditions as repeated measurements, and (b) relative *E(m)*, with each wavelength range of each condition normalized separately.

4. Comparison to literature

The condition-averaged data given in Figure 2(a) was compared to several studies found in the literature [6, 9, 13-22,] as seen in Figure 3. Notwithstanding the wide spread of reported results, the present $E(m)_\lambda$ results show consistency with several previous studies. In particular, the results of Dobbins *et al*. [6] and Schnaiter *et al*. [17] show similar magnitudes, and results of Krishnan *et al*. [19] and Snelling *et al*. [22] compare favourably in terms of spectral variation. This agreement further bolsters the generally accepted notion that soot optical properties are reasonably independent of fuel type, since the present study and the four listed above all use significantly different fuels (crude oil, diesel, various gaseous and liquid fuels, and ethylene, respectively). The results of Köylü and Faeth [20] at the lower wavelengths were also in reasonable agreement, although they showed essentially the opposite trend with increasing wavelength as that found in the present work.

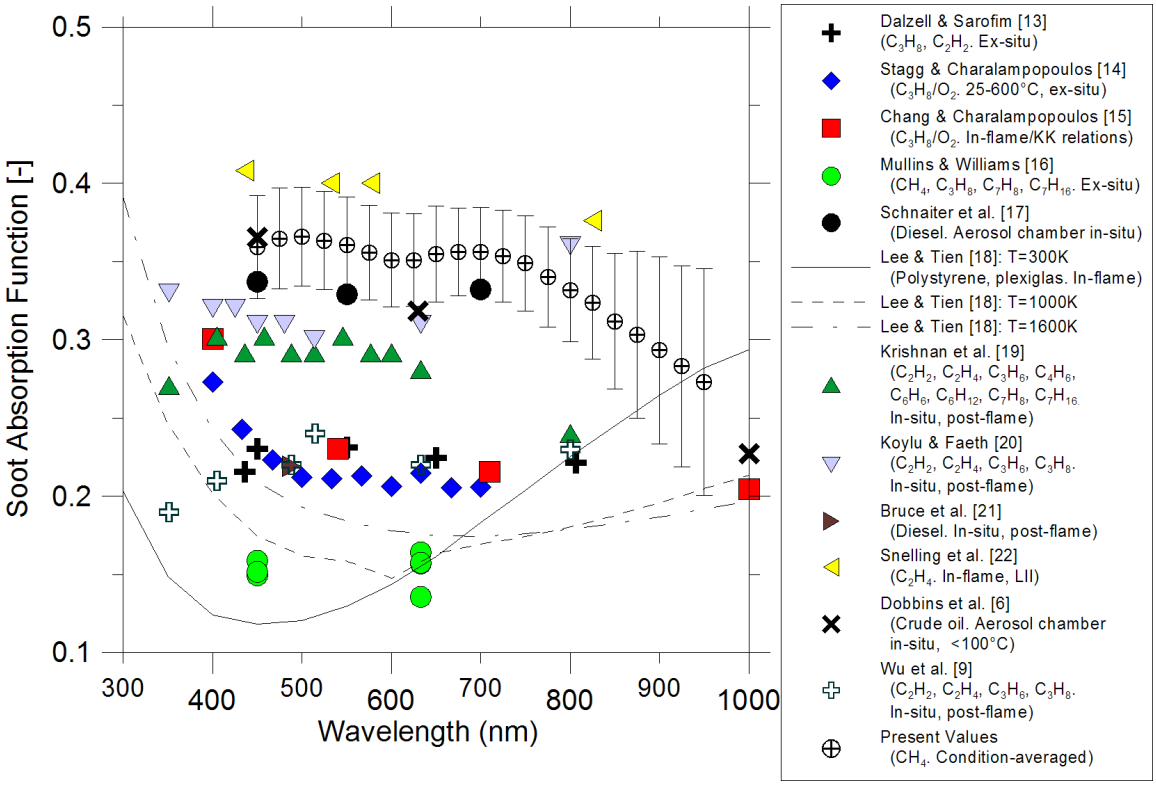

Figure 3: Comparison of present condition-averaged results to values in the literature

The LII data were analyzed using the E(m) results derived through the current work, both in condition-specific and condition-averaged form, to calculate soot volume fractions which were compared with the data obtained gravimetrically. In addition, LII data were analyzed using two popular *E(m)* values from the literature, both assuming constant values over the range of visible wavelengths: *E(m)* = 0.26, derived from the popular value of $m = 1.57 - 0.56i$ for the complex index of refraction generally attributed to Dalzell and Sarofim [23]; and *E(m)* = 0.4, from the work of Snelling *et al*. [22], which is the value currently in use at the NRC. The results of this comparison can be seen in Figure 4. Surprisingly, it is the commonly-used *E(m)* = 0.26 that gives the best agreement in most cases, followed by the present results. The left-most data point and the two right-most data points are exceptions to the general linear trend seen between the gravimetric SVF and that found by LII. The left-most point corresponds to condition C3, which was found to be an outlier throughout this work. The two right-most data points correspond to the fuel-rich "B"-series, showing that these conditions are not well approximated by any of the constant or averaged values. This is perhaps an indication that flame conditions do have an effect on resulting optical properties. The lack of agreement in the soot volume fraction seen by LII and that seen by LOSA could also indicate that

there is some significant difference between the effective absorption properties as seen by these two diagnostics.

5. Conclusions

The absorptive properties of soot were investigated for the twelve burner conditions given in Table 1. Since the variation in the results seen among the tested conditions was small and apparently random, the treatment of these data as repeated measurements was deemed reasonable. The resulting condition-averaged values for *E(m)* and MAC from this work are summarized in Table 2 in 50 nm increments.

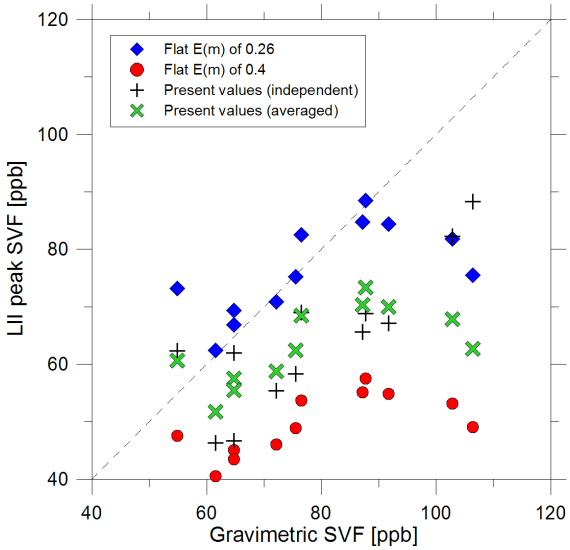

Figure 4: Comparison of LII results using various values for *E(m)*

Table 2: Summary of condition-averaged data in various forms with associated uncertainties

λ [nm]	ρ_{sa}	$U_{\rho sa}$	$E(m)$	$U_{E(m)}$	MAC [m^2/g]	U_{MAC} [m^2/g]
450	0.29	0.06	0.35	0.03	8.0	0.7
500	0.27	0.06	0.36	0.03	7.3	0.6
550	0.25	0.06	0.35	0.03	6.5	0.5
600	0.23	0.05	0.34	0.03	5.8	0.5
650	0.21	0.05	0.35	0.03	5.4	0.4
700	0.20	0.05	0.35	0.03	5.1	0.4
750	0.18	0.05	0.34	0.03	4.7	0.4
800	0.17	0.04	0.33	0.03	4.2	0.4
850	0.15	0.04	0.31	0.04	3.7	0.5
900	0.14	0.04	0.29	0.06	3.7	0.7
950	0.13	0.04	0.27	0.07	3.3	0.8

The results of this work support the idea that the refractive index of soot, and thereby the soot absorption function, is effectively constant across the visible wavelengths (we did observe a consistent dip around 600 nm, though its magnitude is small compared to the uncertainty). This common trend can be observed in Figure 3 for the majority of the studies presented therein. Furthermore, this implies that MAC is inversely proportional to wavelength in the visible range, supporting several similar observations made in the past (e.g., [24] and references therein).

These results also support the idea that soot optical properties are independent of fuel type, as the present results agree well with several previous measurements using widely varying fuels. This conclusion is well-supported by the literature, notably by Mullins and Williams [16], Krishnan *et al*. [19], Köylü and Faeth [20] and Wu *et al*. [9].

Unfortunately, however, LII data analyzed using the present absorption properties under-predicted the soot volume fractions compared to those found by gravimetric analysis. The reasons for this discrepancy are unknown, and further investigation into this effect is recommended.

References

[1] D. Snelling, G. Smallwood, F. Liu, Ö. Gülder, W. Bachalo, Applied Optics 44 (2005) 6773–6785.
[2] H. Michelsen, F. Liu, B. Kock, H. Bladh, A. Boiarciuc, M. Charwath, T. Dreier, R. Hadef, M. Hofmann, J. Reimann, S. Will, P.-E. Bengtsson, H. Bockhorn, F. Foucher, K.-P. Geigle, C. Mounaïm-Rousselle, C. Schulz, R. Stirn, B. Tribalet, R. Suntz, Applied Physics B 87 (2007) 503–521.
[3] A. Coderre, K. Thomson, D. Snelling, M. Johnson, Proceedings of the Combustion Institute / Canadian Section Spring Technical Meeting, 2008, pp. 29–34.

[4] C. Stipe, B. Higgins, D. Lucas, C. Koshland, R. Sawyer, Review of Scientific Instruments 76 (2005) 023908.
[5] A. Coderre, D. Snelling, G. Smallwood, M. Johnson, Proceedings of the Combustion Institute / Canadian Section Spring Technical Meeting, 2007, p. E5.
[6] R. Dobbins, G. Mulholland, N. Bryner, Atmospheric Environment 28 (1994) 889–897.
[7] M. Choi, A. Hamins, G. Mulholland, T. Kashiwagi, Combustion and Flame 99 (1994) 174–186.
[8] M. Choi, G. Mulholland, A. Hamins, T. Kashiwagi, Combustion and Flame 102 (1995) 161–169.
[9] J.-S. Wu, S. Krishnan, G. Faeth, Journal of Heat Transfer 119 (1997) 230–238.
[10] K. Thomson, M. Johnson, D. Snelling, G. Smallwood, Proceedings of the Combustion Institute / Canadian Section Spring Technical Meeting, 2008, pp. 23–28.
[11] A. Brasil, T. Farias, M. Carvalho, Journal of Aerosol Science 30 (1999) 1379–1389.
[12] A. Coderre, Master's thesis, Carleton University (April 2009).
[13] W. Dalzell, A. Sarofim, Journal of Heat Transfer 91 (1969) 100–104.
[14] B. Stagg, T. Charalampopoulos, Combustion and Flame 94 (1993) 381–396.
[15] H. Chang, T. Charalampopoulos, Proceedings of the Royal Society A 430 (1990) 577–591.
[16] J. Mullins, A. Williams, Fuel 66 (1987) 277–280.
[17] M. Schnaiter, H. Horvath, O. Möhler, K.-H. Naumann, H. Saathoff, O. Schöck, Journal of Aerosol Science 34 (2003) 1421–1444.
[18] S. Lee, C. Tien, Proceedings of the 18th International Symposium on Combustion, The Combustion Institute, 1981, pp. 1159–1166.
[19] S. Krishnan, K. Lin, G. Faeth, Journal of Heat Transfer 122 (2000) 517–524.
[20] Ü. Ö. Köylü, G. Faeth, Journal of Heat Transfer 118 (1996) 415–421.
[21] C. Bruce, T. Stromberg, K. Gurton, J. Mozer, Applied Optics 30 (1991) 1537–1546.
[22] D. Snelling, F. Liu, G. Smallwood, Ö. Gülder, Combustion and Flame 136 (2004) 180–190.
[23] K. Smyth, C. Shaddix, Combustion and Flame 107 (1996) 314–320.
[24] T. Bond, R. Bergstrom, Aerosol Science and Technology 40 (2006) 27–67.